Multiaxial fatigue damage modeling of Ti6Al4V alloy

A. K. Marmi[1], A. M. Habraken[1, 2] and L. Duchene[1,2]

[1] **Department ArGEnCo division MS²F, University of Liege, Chemin des Chevreuils, 1, 4000 Liege, Belgium, amarmi@ulg.ac.be, Anne.Habraken@ulg.ac.be, L.Duchene@ulg.ac.be**

[2] **Belgian Scientific research Funds**

ABSTRACT. *The aim of this study is to present a new multiaxial fatigue model based on phenomenological approach for the proportional loading. The model estimations are compared to the classical Lemaitre-Chaboche [1] fatigue model and experimental results. The comparison is done by simulation of SN curves of notched and un-notched forged TA6V samples. To take into account the effect of stress gradient near notch root, the applied loads such as stress amplitude and Von Mises stress are affected by the triaxialty function introduced by Lemaitre [2]. The models enhanced by triaxialty function give correct results for life estimation of notched samples.*

INTRODUCTION

The high-cycle fatigue design of industrial structures is still not resolved especially in the presence of stress concentrations areas (holes, notches,...). A classical fatigue damage model known as NCD (Nonlinear Continuous Damage) advocated by Chaboche based on the concept of damage mechanics was established in 1974. It defines a damage evolution function according to the measured fatigue damage curves. These types of models don't give satisfactory results in the presence of stress gradient in the structures. The aim of the present paper is to develop a more efficient multiaxial fatigue cumulative damage model in the presence of stress gradient effect in the structure. Current state of this model is limited to proportional loading.

ELASTOPLASTIC MODEL

The input data of the fatigue models are the stress fields calculated by FE modeling using a combined nonlinear isotropic/kinematic hardening model with the Von Mises yield surface. The pressure independent yield surface is defined by the function:

$$f = J_2\left(\underline{\sigma} - \underline{\alpha}\right) - R(\overline{\varepsilon}^{pl}) \tag{1}$$

with,

$$J_2(\underline{\sigma}-\underline{\alpha})=\sqrt{\frac{3}{2}(\underline{s}-\underline{\alpha}):(\underline{s}-\underline{\alpha})} \tag{2}$$

where $\underline{s}$ is deviatoric stress tensor and $\underline{\alpha}$ the back-stress tensor.

The hardening law uses two parts: a non linear kinematic hardening one, which describes the translation of the yield surface in stress space through the back-stress $\underline{\alpha}$; and an isotropic hardening one, which describes the change of the equivalent stress defining the size of the yield surface. R is a function of equivalent plastic deformation.

The kinematic hardening part is defined as an additive combination of a purely kinematic term and a relaxation term, introducing the nonlinearity. When temperature and field variable dependencies are omitted, the hardening law can be written as follows:

$$\dot{\underline{\alpha}}=C\frac{1}{R(\bar{\varepsilon}^{pl})}(\underline{\sigma}-\underline{\alpha})\dot{\bar{\varepsilon}}^{pl}-G\underline{\alpha}\dot{\bar{\varepsilon}}^{pl} \tag{3}$$

C, G are material parameters. The isotropic hardening part of the model R, as a function of the equivalent plastic strain $\bar{\varepsilon}^{pl}$

$$R(\bar{\varepsilon}^{pl})=\sigma_y+Q\left(1-e^{-b\bar{\varepsilon}^{pl}}\right) \tag{4}$$

where Q, b are material parameters, σ_y is the yield stress. For the studied material (forged TA6V) C, G, b and Q are identified from the hysteresis strain–stress loops [3] for a strain level of 10^{-2}. To validate the model parameters, FE simulations were performed for different strain amplitudes ($1.4\cdot10^{-2}$, $3\cdot10^{-2}$), the following set of material parameters: σ_y =800 MPa; Q = -150 MPa; b = 10; C = 108380 MPa; G= 350, give a good confrontation between FE modeling and experiences.

LEMAITRE CHABOCHE MODEL

Initially proposed by Chaboche [4] for the uniaxial loading, this model is extended to multiaxial loading by Lemaitre-Chaboche. The increment of the damage by cycle is given by:

$$\delta D=\left[1-(1-D)^{\beta+1}\right]^{\alpha(A_{IIa},\bar{\sigma}_H,\sigma_{VM,\max})}\left[\frac{A_{IIa}}{M_0(1-3b_2\bar{\sigma}_H)(1-D)}\right]^{\beta}\delta N \tag{5}$$

where, A_{IIa}, $\sigma_{VM,\max}$ are respectively the octahedrical amplitude stress “Eq 8” and Von Mises equivalent stress by cycle, $\bar{\sigma}_H$ is the mean hydrostatic stress defined by Sines [5]. β, M_0 , b_2, are material parameters.

The exponent α(..) is given by:

$$\alpha(..) = 1 - a\left\langle \frac{A_{IIa} - A_{II}^{*}}{\sigma_{ul} - \sigma_{VM,\max}} \right\rangle \tag{6}$$

where A_{II}^{*} is multiaxial fatigue strength at 10^7 cycles defined by Sines, σ_u is the yield strength of the material and a is material parameter.

ULG FATIGUE MODEL

The authors propose a fatigue damage model based on Crossland fatigue criterion [6]. The damage increases only if the fatigue damage function f^{Cr} is positive. This function is defined as:

$$f^{\mathrm{Cr}} = \frac{1}{\mathrm{b}}\left(\mathrm{A}_{\mathrm{IIa}} + \mathrm{a}\cdot\sigma_{\mathrm{H,max}} - \mathrm{b}\right) \tag{7}$$

with,

$$\mathrm{A}_{\mathrm{IIa}} = \frac{1}{2}\sqrt{\frac{3}{2}(\mathrm{S}_{\mathrm{ij,max}} - \mathrm{S}_{\mathrm{ij,min}})(\mathrm{S}_{\mathrm{ij,max}} - \mathrm{S}_{\mathrm{ij,min}})} \tag{8}$$

where $S_{ij,max}$ and $S_{ij,min}$ are the maximum and the minimum values of the deviatoric stress tensor during the loading cycle. a and b are material parameters given by:

$$\begin{cases} \mathrm{a} = \dfrac{\tau_{-1} - \dfrac{\mathrm{f}_{-1}}{\sqrt{3}}}{\dfrac{\mathrm{f}_{-1}}{3}} \\ \mathrm{b} = \tau_{-1} \end{cases} \tag{9}$$

with τ_{-1}, f_{-1} the fatigue strength at 10^7 cycles, under alternative torsion and alternative flexion respectively

The following evolution for the damage is assumed:

$$\frac{\mathrm{dD}}{\mathrm{dN}} = \begin{cases} \mathrm{g}(\mathrm{D}, f^{\mathrm{Cr}}) & \text{if} \quad f^{\mathrm{Cr}} > 0 \\ 0 & \text{else} \end{cases} \tag{10}$$

where $g(D, f^{cr})$ is a non linear function depending on the damage variable and the fatigue function by:

$$g(D, f^{Cr}) = \frac{C_1}{\gamma+1} \cdot D^{\alpha_1(...)} \cdot \left(f^{Cr} \right)^{\gamma+1} \tag{11}$$

$$\alpha_1(...) = 1 - n \left\langle \frac{A_{IIa} - A^*_{max}}{\sigma_u - \theta.\sigma_{VM,max}} \right\rangle \tag{12}$$

where n, θ are materials parameters. A^*_{max} is the endurance limit given by Crossland:

$$A^*_{max} = \sigma_{-1} \left(1 - 3 \cdot s \cdot \sigma_{H,max} \right) \tag{13}$$

where σ_{-1} is the fatigue limit of alternative traction-compression loading. s a material parameter.
By integration between D=0 (no damage) to D=1(initiation of macro crack), the number of cycles to failure, Nr can be computed:

$$Nr = \frac{\gamma+1}{C_1 \cdot n} \cdot \left\langle \frac{\sigma_u - \theta.\sigma_{VM,max}}{A_{IIa} - A^*_{max}} \right\rangle \cdot \left(f^{cr} \right)^{-(\gamma+1)} \tag{14}$$

where $C_1 \cdot n = C'$.

THE MODIFIED MODELS

To enhance the estimation of these two models, the effect of the maximal triaxialty function by cycle, $R_{\nu,max}$ was introduced. By replacing the loading parameters A_{IIa}, $\sigma_{VM,\,max}$, $\sigma_{H,max}$ with the following adjusted parameters: $A_{IIa}/\ R_{\nu,max}$, $\sigma_{VM,\,max}/\ R_{\nu,max}$, $\sigma_{H,max}/\ R_{\nu,max}$ was proposed. The triaxialty function is defined by:

$$R_{\upsilon,max} = \frac{2}{3}(1+\nu) + 3(1-2\nu)\left(\frac{\sigma_H}{\sigma_{VM}} \right)^2_{max} \tag{15}$$

where ν is the Poisson modulus.

In the presence of notch, the traxiality increases around the notch root. The adjustment by the traxiality function allows taking into account the effect of this high triaxiality near notch root.

IDENTIFICATION OF MATERIAL PARAMETERS OF THE MODELS

The smooth fatigue data [7] were obtained from 73 uniaxial strain-controlled (LCF) and load-controlled (HCF) specimens tested over a range of stress ratios. The results of this smooth bar testing were used to identify the models parameters. The curves of Fig. 1. compare the experimental data for unnotched plate specimens (Kt = 1) with R = 0.5, R = 0.1 and R=-1 with ULg model estimation.

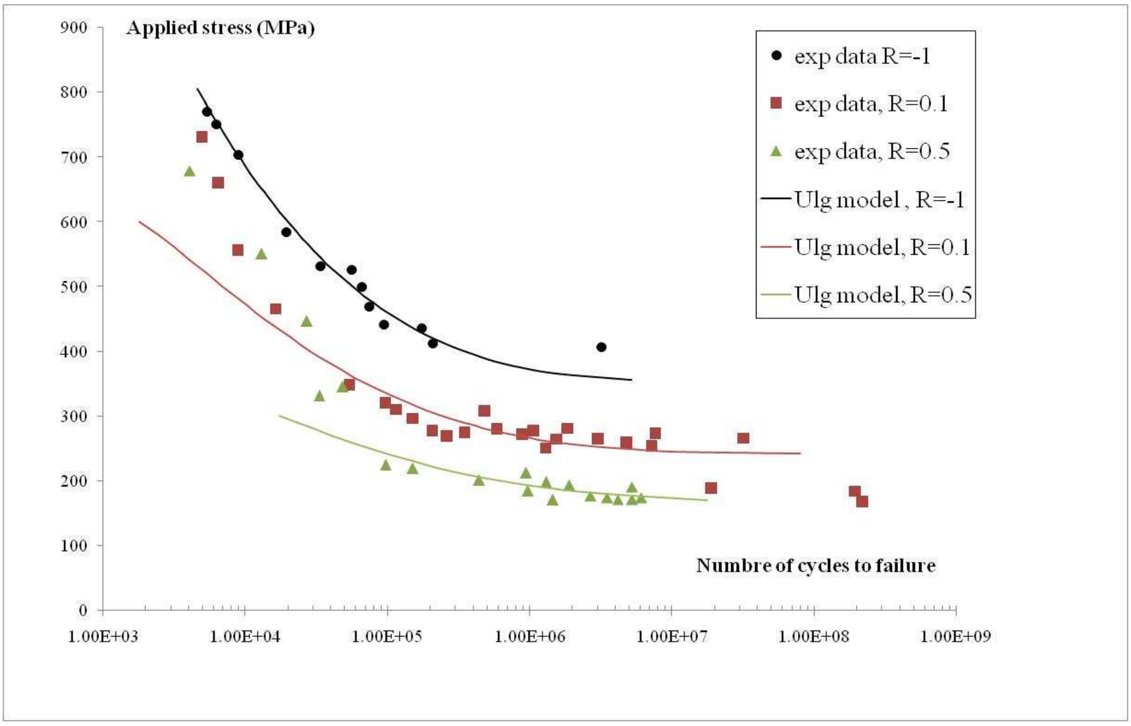

Figure 1. Experimental and estimated SN curves FE simulation, for R = 0.1, 0.5, -1. Unnotched specimen, 1D loading.

The materials parameters are taken from the best fit of the experimental SN curves. The values of the material parameters are given in Table 1 and Table 2.

LEMAITRE- CHABOCHE MODEL

Table 1. Material parameters of the Lemaitre and Chaboche fatigue damage model.

b_1 (MPa^{-1})	b_2 (MPa^{-1})	β	$aM_0^{-\beta}$	σ_{l0} (MPa)	σ_{ul} (MPa)
0.00120	0.00085	7.689	4.10E-28	395	1085

ULG MODEL

Table 2. Material parameters of the ULg fatigue damage model.

a	b (MPa)	γ	C'	θ	s (MPa^{-1})	σ_{-1} (MPa)	σ_u (MPa)
0.467	220	0.572	7.12E-05	0.75	0.00105	350	1199

One can observe that the yield strength of the material has been optimised to provide good fatigue estimation, it keeps however the order magnitude of the material yield strength.

EXPERIMENTAL RESULTS ON Ti-6Al-4V NOTCHED SPECIMENS

Rajiv et al. [8] have performed fatigue tests on specimens of forged TA6V. The fatigue specimens were machined from Ti–6Al–4V forged plates. The alpha–beta titanium alloy microstructure consisted of approximately 60% alpha phase with the remainder lamellar transformed beta phase. Double-edge notched fatigue specimens with a stress concentration factor, Kt=2.68, and a notch radius, ρ=0.53 mm. The thickness of the plate is 3.65 mm. The HCF data were obtained at a frequency of 60 Hz for stress ratios, R=-1, 0.1, and 0.5. The measured yield stress of the material is 930 MPa and the yield strength is 1009 MPa

FE MODELING OF RAJIV TESTS

The home-made finite element code Lagamine [9] was used. The first step in the numerical computations was the determination of the mesh density required at the notch root to obtain a converged solution independent of the mesh size. This analysis was performed in elasticity with two element layers through the thickness. The final mesh consisted of 1192 BWD3D [10] finite elements “Fig 2”.

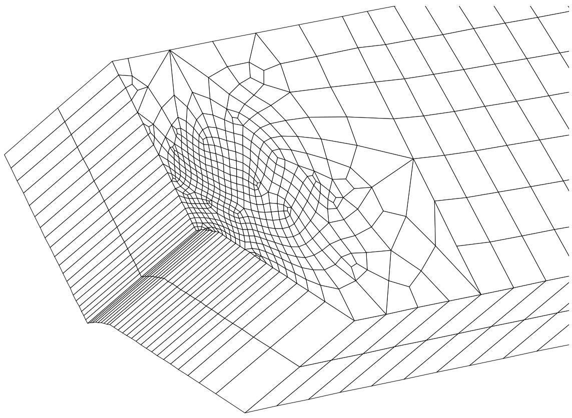

Figure 2. Finite element mesh for the V-notched specimen (only one eighth is modelled due to symmetry).

RESULTS AND DISCUSSION

Due to the presence of the stress gradient around the notch root, the estimation of the ULg model and Lemaitre-Chaboche (identified on smooth tests) without modification under estimate the fatigue life for notched specimens. The modified models give an enhancement of the fatigue life evaluation “Eq 15”. The effect of the triaxialty is included in the modified models “Figs 3, 4 and 5”

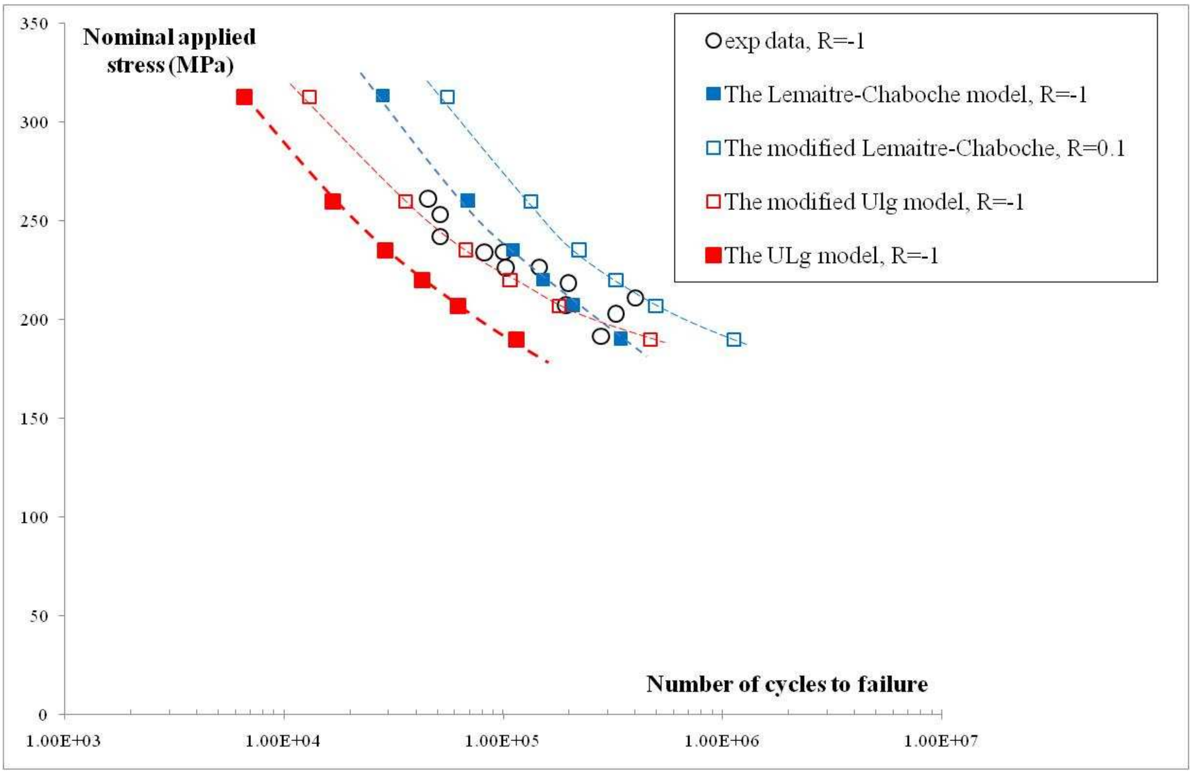

Figure 3. Experimental and estimated SN curves, for R = -1, V-notched specimen, Kt=2.68

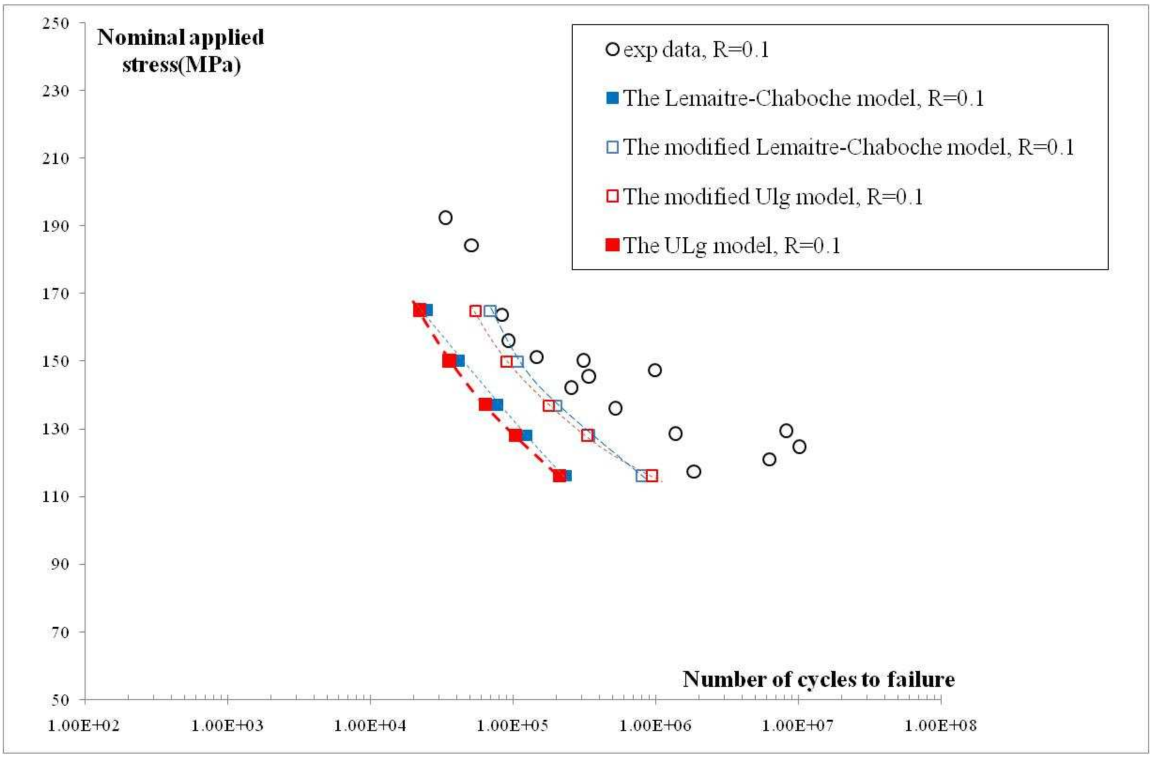

Figure 4. Experimental and estimated SN curves, for R = 0.1, V-notched specimen, Kt=2.68

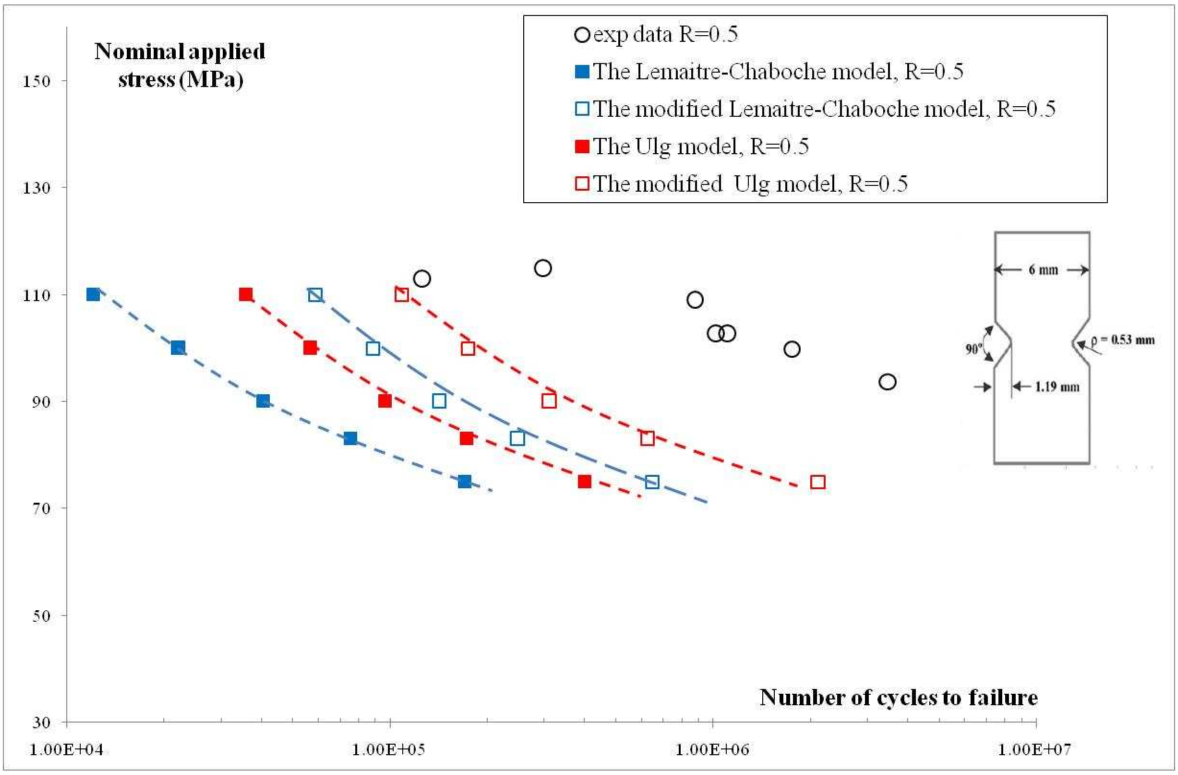

Figure 5. Experimental and estimated SN curves, for R = 0.5, V-notched specimen, Kt=2.68

CONCLUSION

In this study, the finite element method was used to obtain an accurate description of the stress field around the geometrical defect (a V-notch) of the tensile specimens. The FE results were used as input data for the Lemaitre and Chaboche continuum damage model and ULg model in order to estimate the material fatigue behaviour. Classical mechanical tests and uniaxial fatigue tests (cyclic tensile tests on the unnotched specimens) were used to fit the material parameters Afterwards, the selected models and the identified parameters were validated on the simulations of multiaxial fatigue tests (cyclic tensile tests on the V-notched).
The triaxialty function is an easy way to take in account the effect of the triaxialty around the notch root. The modified models do not need new parameters as usually introduced when stress gradient is taken into account [8, 11]. The efficiency of this approach has also been checked on other experimental results (smooth test on a plate and notch tests with Kt=1.5, 2, 4 and R=0, 0.2 of aluminum alloy and inconel 718) [12].

REFERENCES

1. Lemaitre Jean, Chaboche Jean-Louis. Mechanics of solid materials. New ed. Cambridge University Press; 1994.

2. J.Lemaitre and I. Doghri, (1994), *Damage 90: a post processor for crack initiation, Comput. Methods Appl. Engrg.* **115 pp. 197–232**

3. Boyce BL, Chen X, Peters JO, (2003) Hutchinson JW, Ritchie RO, *Mechanical relaxation of localized residual stresses associated with foreign object damage. Mater Sci Eng*; **A349:48–58.**

4. Chaboche, J. L., Lesne P. M., (1988), *non-linear continuous fatigue damage model, Fatigue & fracture of engineering materials & structures*, **vol. 11, no1,1-17.**

5. Sines G. (1959), *Behavior of metals under complex static and alternating stresses, In: Sines G, Waisman JL, editors. Metal fatigue. New York: McGraw Hill*; **p. 145–69.**

6. B. Crossland (1956), *Effect of large hydrostatic pressures on the torsional fatigue strength of an alloy steel. – Actes de "The international conference on fatigue of metals", Institution of mechanical engineers, London,* **Pages 138-149**

7. Kallmeyer AR, Krgo A, Kurath P. (2002), *Evaluation of multiaxial fatigue life prediction methodologies for Ti–6Al–4V. ASME J Eng Mater Technol*; **124(2):229–37.**

8. Rajiv A. Naik, David B. Lanning (2005), *Theodore Nicholas, Alan R. Kallmeyer, A critical plane gradient approach for the prediction of notched HCF life, International Journal of Fatigue,* **Volume 27, Issue 5, Pages 481-492**

9. Duchene L, Lelotte T, Flores P, Bouvier S, Habraken AM. (2008), *Rotation of axes for anisotropic metal in FEM simulations. Int J Plasticity*; **24:397–427.**

10. Duchêne L, de Montleau P, El Houdaigui F, Bouvier S, Habraken AM, (2005), *Analysis of texture evolution and hardening behavior during deep drawing with an improved mixed type FEM element. In: Smith LM, Pourboghrat F, Yoon JW, Stoughton TB, editors*. **Proceedings of the 6th international NUMISHEET**

11. A.K. Marmi, A.M. Habraken, L. Duchêne (2009), *Multiaxial fatigue damage modelling at macro scale of Ti6Al4V alloy, International Journal of Fatigue*. **vol. 31, nº 11-12, pp. 2031-2040**

12. A.K. Marmi, A.M. Habraken, (2010), *Calcul de la durée de vie des éprouvettes entaillées par l'utilisation de la fonction de triaxialité Rv*, **Rapport interne 2010-1**.